J. Phys. Chem. A **1999,** *103,* 4948−4954

Rotational Spectra, Molecular Structure, and Electric Dipole Moment of Propanethial *S*-Oxide

Jennifer Z. Gillies* and Elizabeth Cotter

Department of Chemistry, Siena College, Loudonville, New York 12211

Charles W. Gillies and Hugh E. Warner

Department of Chemistry, Rensselaer Polytechnic Institute, Troy, New York 12180

Eric Block

Department of Chemistry, State University of New York at Albany, Albany, New York 12222

Received: January 21, 1999

Pulsed-beam Fourier transform microwave spectroscopy was used to study propanethial *S*-oxide (**1**), an unstable species generated in a (*Z*)/(*E*) ratio of 98/2 by pyrolysis of 2-methyl-2-propyl-1′-propenyl vinyl sulfoxide at 350 °C in Ar or Ne/He gas flows. A fit of 25 transition frequencies to a Watson "*A*" reduced Hamiltonian gave the following rotational constants and centrifugal distortion constants for the normal isotopomer of (*Z*)-**1a**: $A = 10\,182.2558(3)$ MHz, $B = 2209.5000(9)$ MHz, $C = 1997.1734(8)$ MHz, $\Delta_{JK} = -62.69(2)$ kHz, $\Delta_J = 4.165(3)$ kHz, $\delta_J = 0.3336(3)$ kHz and $\delta_K = -31.7(4)$ kHz. Twelve transitions were fit in the same manner for (*E*)-**1b** to give $A = 16231(86)$ MHz, $B = 1823.6154(7)$ MHz, $C = 1785.7215(7)$ MHz, $\Delta_{JK} = -12.5(5)$ kHz, $\Delta_J = 0.48(1)$ kHz, $\delta_J = -0.060(8)$ kHz. Microwave spectra of six (*Z*) isotopomers were assigned and a partial substitution structure was derived: $r(\mathrm{C{=}S}) = 1.585(6)$ Å, $r(\mathrm{S{-}O}) = 1.473(2)$ Å, $r(\mathrm{{=}CH{-}CH_2}) = 1.513(7)$ Å, $r(\mathrm{CH_3{-}CH_2}) = 1.536(3)$ Å, $\theta(\mathrm{CSO}) = 113.8(2)°$, $\theta(\mathrm{CCS}) = 126.7(3)°$, and $\phi(\mathrm{CCCS}) = 118.4°$. The electric dipole moment components of the (*Z*) isomer along the *a*, *b*, and *c* principal axes were measured to be $\mu_a = 2.59(2)$ D, $\mu_b = 2.11(2)$ D, and $\mu_c = 0.33(6)$ D, respectively, which gives a total electric dipole moment of 3.35(2) D.

I. Introduction

Thial *S*-oxides have the structure $\mathrm{RCH{=}S^{+}{-}O^{-}}$ and are the sulfur analogues of carbonyl oxides, $\mathrm{RCH{=}O^{+}{-}O^{-}}$. The high reactivity of this class of organosulfur compounds makes study difficult. They have been investigated spectroscopically in the gas phase by pumping an appropriate sulfoxide precursor through a hot zone and then into the absorption cell of the spectrometer.[1] The first report of the parent species, methanethial *S*-oxide (CH_2SO), used microwave spectroscopy to characterize the compound and determine that it has a planar gas-phase geometry.[1] Propanethial *S*-oxide (CH_3CH_2CHSO) plays an important role in Allium chemistry. There is considerable evidence that indicates it is the lachrymatory factor responsible for tearing when an onion is cut.[2] Recently, propanethial *S*-oxide was detected in the vapor above chopped onions by a direct in situ spectroscopic technique.[3] Freshly chopped onions were placed in a tube and the volatile gases carried in Ne/He to a modified solenoid gas valve which sampled the gas mixture for analysis in the Fabry−Perot cavity of a Fourier transform microwave spectrometer.[3] The high resolution and molecular isotopic specificity of the Fourier transform microwave technique provided an unambiguous way to identify the site of deuterium incorporation in propanethial *S*-oxide obtained from an onion−D_2O homogenate. This isotopic study was used to elucidate the mechanism of the formation of propanethial S-oxide from the process of cutting onions.[3]

To use the in situ method described above analytically, it was necessary to observe and assign the rotational spectrum of propanethial *S*-oxide. As shown in Figure 1, (*Z*) and (*E*) configurations of propanethial *S*-oxide, **1a**, **1b**, arise from geometrical isomerization about the C═S bond. The spectroscopic problem is further complicated by the possibility of rotational isomerism of the ethyl group relative to CHSO. This paper reports the microwave spectroscopic data and assignments which support the chemical results discussed above for (*Z*)- and (*E*)-propanethial *S*-oxide. The rotational spectra were recorded by producing propanethial *S*-oxide in a Ne/He flow by pyrolysis of 2-methyl-2-propyl-1′-propenyl sulfoxide, **2**. A similar pyrolytic method has been used in an analogous study of the rotational spectra of (*Z*)- and (*E*)-ethanethial *S*-oxide, **3a**, **3b**.[4] Spectra of six isotopomers of the (*Z*) configuration were assigned and a heavy atom structure was obtained from the effective moments of inertia. In addition, a weak spectrum was assigned to the (*E*) configuration, which is formed in much lower

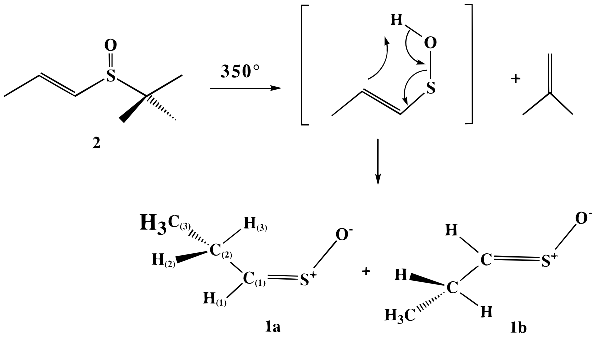

Figure 1. (*Z*) **1a** and (*E*) **1b** geometrical isomers of propanethial *S*-oxide shown for the skew conformations.

10.1021/jp9902506 CCC: $18.00

concentration from the pyrolysis. The molecular structures of **1a**, **1b** are compared to the known structures of methanethial *S*-oxide,[1] **3a**,[4] and related molecules. The molecular Stark effect was used to obtain the electric dipole moment of the normal isotopomer of **1a**.

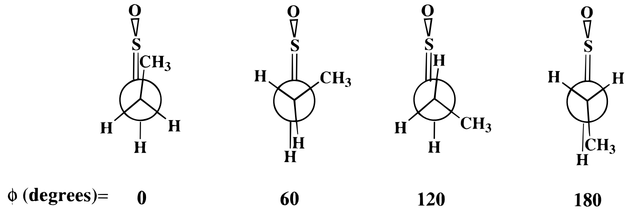

Figure 2. Rotational isomers of **1a** defined by the dihedral angle, ϕ(CCCS) = 0, 60, 120, and 180° corresponding to the cis, gauche, skew, and trans conformations, respectively.

TABLE 1: Observed Rotational Transitions of 1a, (*Z*)-CH_3CH_2CHSO, and (*Z*)-$CH_3CH_2CH^{34}SO$, and 1b, (*E*)-CH_3CH_2CHSO

transition	(*Z*)-CH_3CH_2-CHSO		(*Z*)-CH_3-$CH_2CH^{34}SO$		(*E*)-CH_3CH_2-CHSO	
$J'_{K-1,K+1}-J''_{K-1,K+1}$	ν_{obsd}[a] (MHz)	$\Delta\nu$[c]	ν_{obsd}[b] (MHz)	$\Delta\nu$[c]	ν_{obsd}[a] (MHz)	$\Delta\nu$[c]
$1_{10}-1_{01}$	8 185.2707	0.9	8 141.183	−4.2		
$2_{12}-1_{11}$	8 201.0218	0.2	8 098.959	0.4	7 180.8133	0.3
$2_{11}-2_{02}$	8 402.1566	−0.8	8 355.050	2.2		
$2_{02}-1_{01}$	8 409.0190	−0.4	8 304.136	−2.2	7 218.5840	0.0
$2_{11}-1_{10}$	8 625.9066	−0.3	8 518.001	2.2	7 256.5999	−4.7
$3_{12}-3_{03}$	8 735.2838	0.0	8 683.463	0.8		
$4_{13}-4_{04}$	9 193.8616	0.1				
$4_{04}-3_{13}$	9 323.0876	−0.1				
$5_{14}-5_{05}$	9 789.8403	0.3				
$6_{15}-6_{06}$	10 537.4354	−0.1				
$7_{16}-7_{07}$	11 452.3470	−0.1				
$1_{11}-0_{00}$	12 179.4755	−0.4	12 085.827	−0.5		
$3_{13}-2_{12}$	12 298.6981	0.5	12 145.669	0.3	10 771.1409	0.1
$8_{17}-8_{08}$	12 550.5997	0.1				
$3_{03}-2_{02}$	12 602.8070	−0.2	12 445.728	1.3	10 827.6605	−0.3
$3_{22}-2_{21}$	12 621.0760	1.0	12 463.556	1.9		
$3_{21}-2_{20}$	12 637.8379	−0.2	12 479.943	−3.3		
$3_{12}-2_{11}$	12 935.9341	0.4	12 774.139	−2.2	10 884.8380	2.8
$5_{05}-4_{14}$	13 877.9873	0.4				
$2_{12}-1_{01}$	16 173.8406	−0.1	16 030.620	1.7		
$4_{14}-3_{13}$	16 393.0461	0.4	16 189.128	0.6	14 361.3748	−0.4
$4_{04}-3_{03}$	16 783.7989	−0.5	16 574.805	−1.0	14 436.4796	0.4
$4_{23}-3_{22}$	16 824.3402	−0.6				
$4_{22}-3_{21}$	16 866.1682	−0.1				
$4_{13}-3_{12}$	17 242.3767	−0.4	17 026.787	1.0	14 512.9813	1.7
$5_{15}-4_{14}$					17 951.4821	0.2
$5_{05}-4_{04}$					18 044.9531	−0.1
$5_{14}-4_{13}$					18 141.0078	−1.2

[a] The frequency measurements have an estimated uncertainty of 2 kHz. [b] The frequency measurements have an estimated uncertainty of 4 kHz. [c] $\Delta\nu$ is the observed minus calculated frequency from the least-squares fit, expressed in kHz.

II. Experimental Section

The synthesis of the pyrolytic precursor, 2-methyl-2-propyl-1′-propenyl sulfoxide **2**, has been described previously.[3] A sample of **2** was transferred to a steel trap and pressurized to about 20 psi above atmospheric pressure with spark gas (∼80% neon/∼20% helium). The gas output from the trap flowed through a 1 mm i.d. 30 cm long quartz tube inserted into a tube furnace. The volatile pyrolysis products exiting the furnace were then swept through a dual flow pulse valve described previously,[5] which sampled the gas flow for analysis in the cavity of the spectrometer. A continuous flow of products through the valve was maintained by leading the normal output of the valve to a bubbler before being exhausted into a hood. Optimal spectral intensity was obtained by using the following conditions: precursor trap temperature of 60 °C, furnace temperature of 350 °C, and a flow rate of 2−5 mL/min. The intensity of the known rotational spectrum of isobutylene,[6] which is another pyrolysis product of **2**, was optimized prior to the initiation of spectral searches for the normal isotopomer of **1a**. At least 4 h of surface conditioning of the entire flow system was sometimes required to observe the spectrum of **1a**. To incorporate deuterium into **1a**, a gas cylinder containing ∼20 mL of D_2O was pressurized with spark gas or argon to 80 psi. This mixture then flowed through the precursor trap and into the pyrolysis region as described above. These methods have been described recently in an investigation of the rotational spectra of **3a**, **3b**.[4]

The spectral data reported for **1a**, **1b** were recorded with a pulsed-beam Fourier transform microwave spectrometer[7] of the Balle-Flygare design.[8] Instrumental improvements to the spectrometer have been described in a recent publication.[4] The normal isotopomers of the (*Z*) and (*E*) configurations as well as the (*Z*)-$CH_3CHDCHSO$ isotopomer were measured with the new system.[4] The estimated precision of transition frequency measurements with this system is typically less than 2 kHz. All the less abundant isotopomers of **1a** were observed prior to the instrumental improvements, and the line frequencies have an estimated measurement precision of 4 kHz. The method used for electric dipole moment measurements is described in the literature.[9,10] Briefly, a pulsed flow valve oriented perpendicular to the cavity axis introduces gas pulses into the region of a dc electric field. This dc field is oriented parallel to the microwave electric field in the cavity. The electric dipole is determined by observing frequency shifts of the $\Delta M_J = 0$ transitions at a number of values of the dc electric field. The dc plate separation was determined by calibration using the $J = 1-0$ transition of OCS and its measured electric dipole moment of 0.71519(3) Debyes.[11]

III. Spectral Analysis

Spectral predictions generated for **1a**, **1b** utilized the structure of CH_2SO to approximate the OCS angle and the bond distances[1] and assumed a typical hydrocarbon geometry for the ethyl group. The methylene carbon adjacent to the sp^2-hybridized carbon was fixed in the CSO plane for **1a**, **1b**. A number of different rotameric forms were considered by varying the SCCC dihedral angle. As shown in Figure 2, the methyl carbon is positioned cis and trans with respect to the CCSO plane for dihedral angles of ϕ(SCCC) = 0 and 180°, respectively. Gauche and skew conformations are obtained when the methyl carbon is rotated out of the CCSO plane. All of these structures are predicted to exhibit nearly prolate asymmetrical top spectra with predominately *a*- and *b*-type selection rules. The (*Z*) configuration is less prolate than the (*E*) isomer because the OSCCC backbone of the molecule is less extended for the (*Z*) isomer.

A very intense *a*-type spectrum was observed first in the spectral search for the normal isotopomer of **1a**. The initial assignment was obtained by identifying the $J = 3_{03}-2_{02}$ transition at 12 602.8070 MHz, followed by the $3_{22}-2_{21}$ and $3_{21}-2_{20}$ transitions at 12 621.0760 and 12 637.8379 MHz, respectively. Then, the harmonic relation, $\nu \cong (B + C)(J + 1)$ was used to find the $4_{04}-3_{03}$ and $2_{02}-1_{01}$ $K_{-1} = 0$ lines. A total of 13 *a*-type transitions were measured and their frequencies used to obtain preliminary values of the rotational constants. These constants were accurate enough to closely predict the frequencies of the *b*-type lines. In total, 25 transition frequencies were measured and least-squares fit to an I^r, *A*-reduced,

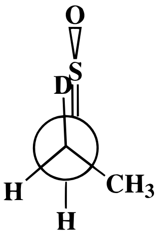

Figure 3. Observed monodeuterated isotopomer of **1a**, (*Z*)-CH_3-CHDCHSO; the Newman projection views along the methylene carbon−sulfine carbon bond (C_2−C_1). For this configuration the deuterium falls almost in the OSC_1C_2 plane.

TABLE 2: Rotational and Centrifugal Distortion Constants of 1a, (*Z*)-CH_3CH_2CHSO, (*Z*)-$CH_3CH_2CH^{34}SO$, and 1b, (*E*)-CH_3CH_2CHSO

	(*Z*)-CH_3CH_2CHSO	(*Z*)-$CH_3CH_2CH^{34}SO$	(*E*)-CH_3CH_2CHSO
A (MHz)	10 182.2558(3)[a]	10 113.396(1)	16 231(86)
B (MHz)	2209.5000(9)	2181.7936(8)	1823.6154(7)
C (MHz)	1997.1734(8)	1972.3903(5)	1785.7215(7)
Δ_{JK} (kHz)	−62.69(2)	−59.80(9)	−12.5(5)
Δ_J (kHz)	4.165(3)	4.01(1)	0.48(1)
δ_J (kHz)	0.3336(3)	0.31(1)	−0.060(8)
δ_K (kHz)	−31.7(4)	−31.7[e]	
σ (kHz)[b]	0.5	2.5	2.4
κ[c]	−0.948 12	−0.948 56	−0.994 75
Δ (u·Å^2)[d]	−25.316 20	−25.379 23	−25.254 95

[a] Quantities in parentheses are one standard deviation. [b] σ is the overall standard deviation of the least-squares fit. [c] κ, the asymmetry parameter, is equal to $(2B - A - C)/(A - C)$. [d] $\Delta = I_c - I_a - I_b$ is the inertia defect. [e] The parameter is fixed to this value in the least-squares fit.

TABLE 3: Observed Rotational Transitions of 1a, (Z)-$CH_3CH_2{}^{13}CHSO$, (Z)-$CH_3{}^{13}CH_2CHSO$, and (Z)-$^{13}CH_3CH_2CHSO$

transition	(Z)-$CH_3CH_2{}^{13}$-CHSO		(Z)-$CH_3{}^{13}CH_2$-CHSO		(Z)-$^{13}CH_3CH_2$-CHSO	
$J'_{K-1,K+1}$−$J''_{K-1,K+1}$	ν_{obsd}[a] (MHz)	$\Delta\nu$[b]	ν_{obsd}[a] (MHz)	$\Delta\nu$[b]	ν_{obsd}[a] (MHz)	$\Delta\nu$[b]
1_{10}−1_{01}			8 125.556	−2.8		
2_{12}−1_{11}	8 184.022	−0.6	8 132.707	−1.6		
2_{02}−1_{01}	8 395.877	−1.1	8 334.686	−1.0	8 184.062	1.2
2_{11}−2_{02}			8 335.979	−0.4		
2_{11}−1_{10}	8 617.088	0.6	8 545.107	−0.6	8 388.154	−0.8
1_{11}−0_{00}	12 049.064	−6.5	12 088.735	2.4	12 084.444	−2.3
3_{13}−2_{12}	12 273.052	−5.4	12 196.363	−2.2	11 979.322	−2.8
3_{03}−2_{02}	12 582.527	3.0	12 491.856	0.7	12 266.568	0.6
3_{12}−2_{11}	12 922.562	0.9	12 814.888	2.6	12 579.618	0.8
2_{12}−1_{01}	16 032.899	6.5	16 052.059	0.8	15 978.417	2.3
4_{14}−3_{13}	16 358.602	1.0	16 256.860	1.3	15 967.766	1.0
4_{04}−3_{03}	16 755.697	−0.1	16 636.876	−0.9	16 337.701	−0.4
4_{13}−3_{12}	17 224.272	−0.9	17 081.265	−0.7	16 767.882	−0.2

[a] The frequency measurements have an estimated uncertainty of 4 kHz. [b] $\Delta\nu$ is the observed minus calculated frequency from the least-squares fit expressed in kHz.

TABLE 4: Observed Rotational Transitions of 1a, (Z)-$CH_3CHDCHSO$

transition		(*Z*)-$CH_3CHDCHSO$	
$J'_{K-1,K+1}$−$J''_{K-1,K+1}$	*F′*-*F″*	ν_{obsd}[a] (MHz)	$\Delta\nu$[b](kHz)
1_{10}−1_{01}	2−2	7 808.0401	−0.5
2_{11}−2_{02}	2−2	8 030.9256	−1.4
	3−3	8 030.9534	−0.2
2_{12}−1_{11}	1−1	8 142.7910	2.4
	2−1	8 142.8287	0.2
	3−2	8 142.8425	−0.5
	1−0	8 142.8890	0.2
2_{02}−1_{01}	1−0	8 356.0249	−1.8
	3−2	8 356.0417	−0.1
3_{12}−3_{03}	3−3	8 373.9094	−0.7
	4−4	8 373.9436	0.1
	2−2	8 373.9572	2.1
2_{11}−1_{10}	2−1	8 578.9373	1.5
	3−2	8 578.9548	0.0
4_{13}−4_{04}	4−4	8 847.1514	−0.2
	5−5	8 847.1900	0.9
1_{11}−0_{00}	0−1	11 770.2991	0.4
	2−1	11 770.3587	−0.1
	1−1	11 770.3977	−1.2
3_{13}−2_{12}	4−3	12 211.1678	−0.7
	2−1	12 211.1760	1.1
3_{03}−2_{02}	4−3	12 522.2573	−0.5
3_{22}−2_{21}	3−2	12 542.0858	0.1
	4−3	12 542.1027	−0.2
3_{21}−2_{20}	3−2	12 560.6108	0.1
	4−3	12 560.6275	−2.2
	2−1	12 560.6407	1.1
3_{12}−2_{11}	3−2	12 865.2404	−1.4
	4−3	12 865.2480	0.4
5_{05}−4_{14}	5−4	14 140.8430	−0.5
	6−5	14 140.8759	−0.5
	4−3	14 140.8854	1.2
2_{12}−1_{01}	3−2	15 732.8150	0.3
	2−1	15 732.8573	0.8
4_{14}−3_{13}	5−4	16 275.8688	0.6
4_{04}−3_{03}	5−4	16 674.3964	0.2
4_{23}−3_{22}	4−3	16 718.7292	−0.6
	5−4	16 718.7372	0.3
4_{22}−3_{21}	4−3	16 764.9450	−0.7
	5−4	16 764.9557	0.8
4_{13}−3_{12}	5−4	17 147.6413	−0.5

[a] The frequency measurements have an estimated uncertainty of 2 kHz. [b] $\Delta\nu$ is the observed minus calculated frequency from the least-squares fit.

asymmetrical top, Watson Hamiltonian.[12] The transition frequencies and assignments are reported in Table 1 and the spectral constants from the least-squares fit are listed in Table 2. All but the four *a*-type $K_{-1} = 2$ lines could be fit to the estimated frequency measurement uncertainty of less than 2 kHz with the three quartic centrifugal distortion constants, Δ_J, Δ_{JK}, and δ_J. A fourth distortion constant, δ_K was needed when the four $K_{-1} = 2$ lines were included in the fit. The large inertial defect of −25.316 20 μÅ^2 calculated from the experimental moments of inertia is consistent only with the skew structural models. κ, the asymmetry parameter, is found to be −0.948 12 from the rotational constants listed in Table 2, which indicates the spectrum arises from **1a** rather than **1b**. Microwave spectra observed for the ^{34}S and ^{13}C isotopomers unambiguously show the normal isotopomer lines listed in Table 1 are from **1a** not **1b**.

The spectra of the ^{34}S and the three singly substituted ^{13}C isotopomers were observed in natural abundance. Strategies for the assignments of these isotopomers followed the same procedures outlined above for the normal isotopic species. In each case, the *a*-type transitions were assigned first and the spectral constants from the *a*-type fits were used to predict the frequencies of the *b*-type lines. Table 1 contains the frequencies of the sixteen transitions that were measured for the ^{34}S isotopomer. Ten transitions were measured for the isotopomer with ^{13}C substitution at the terminal carbon, thirteen for substitution at the central carbon, and eleven for the substitution at the carbon bonded to the sulfur. The transition frequencies of the ^{13}C isotopomers are listed in Table 3. Spectral constants calculated from least-squares fits of the measured line frequencies using the Watson Hamiltonian are given in Table 5. For the four isotopomers, the three quartic centrifugal distortion constant, Δ_J, Δ_{JK}, and δ_J were fit and the fourth distortion constant, δ_K, was fixed at the value determined for the normal isotopomer.

TABLE 5: Spectral Constants of 1a Isotopomers (*Z*)-$CH_3CH_2{}^{13}CHSO$, (*Z*)-$CH_3{}^{13}CH_2CHSO$, (*Z*)-${}^{13}CH_3CH_2CHSO$, and (*Z*)-$CH_3CHDCHSO$

	$CH_3CH_2{}^{13}$-CHSO	$CH_3{}^{13}CH_2$-CHSO	${}^{13}CH_3CH_2$-CHSO	CH_3CHD-CHSO
A (MHz)	10 057.122(5)[a]	10 107.033(1)	10 137.426(3)	9789.1005(3)
B (MHz)	2208.316(2)	2187.7397(7)	2146.981(1)	2199.177(1)
C (MHz)	1991.901(2)	1981.6571(5)	1946.973(1)	1981.223(1)
Δ_{JK} (kHz)	−63.3(6)	−60.2(2)	−63.1(3)	−54.80(3)
Δ_J (kHz)	4.14(3)	3.98(1)	4.04(2)	3.846(5)
δ_J (kHz)	0.31(3)	0.28(1)	0.32(2)	0.189(4)
δ_k (kHz)	−31.7[e]	−31.7[e]	−31.7[e]	−26.4(6)
χ_{aa} (kHz)				−54(1)
χ_{bb}-χ_{cc} (kHz)				213(2)
σ (kHz)[b]	5.0	2.2	2.4	1.1
κ[c]	−0.946 33	−0.949 27	−0.951 16	−0.944 17
Δ (u·Å^2)[d]	−25.386 55	−25.979 32	−25.671 69	

[a] Quantities in parentheses are one standard deviation. [b] σ is the overall standard deviation of the least-squares fit. [c] κ, the asymmetry parameter, is equal to $(2B - A - C)/(A - C)$. [d] $\Delta = I_c - I_a - I_b$ is the inertia defect. [e] Fixed at the value determined for (*Z*)-CH_3CH_2CHSO.

Deuterium was incorporated into **1a** by pyrolyzing **2** in the presence of D_2O. Since the site of deuterium substitution in **1a** via this reaction was not certain, microwave spectra of all possible monodeuterated species of **1a** were calculated using a structure determined from the rotational constants measured for the five isotopomers described above. The spectrum of only one deuterated isotopomer was observed, (*Z*)-$CH_3CHDCHSO$, despite extensive searches in the frequency regions calculated for intense low J lines of the other monodeuterated isotopomers. For the assigned isotopomer, the deuterium is bonded to the methylene carbon and is located at a site that falls nearly in the OSCC plane (see Figure 3). Forty-one hyperfine components of twenty *a*- and *b*-type transitions were observed and the measured line positions were iteratively fit using the asymmetric top Watson Hamiltonian with one quadrupolar nucleus.[13] Table 4 lists the measured transition frequencies and residuals from the least-squares fit. The spectral constants determined from the fit including the four quartic centrifugal distortion constants, Δ_J, Δ_{JK}, δ_J, and δ_K and the deuterium quadrupole coupling constants, χ_{aa} and $\chi_{bb} - \chi_{cc}$, are given in Table 5. The overall standard deviation of 1.1 kHz obtained for the fit is within the measurement precision of 2 kHz estimated for the weakest hyperfine transitions.

From NMR studies, it is found that a vacuum pyrolysis of **2** produces **1a** and **1b** in a ratio of 98/2.[3] Since the carbon-13 isotopomers of **1a** were observed in natural abundance (1.1%), an attempt was made to observe the normal isotopomer spectrum of **1b**. The model structure calculations described above indicated **1b** is more prolate than **1a**. κ was computed to be −0.996 for **1b** compared to −0.95 for **1a** and a number of intense *a*-type transitions are expected in the spectral range of the spectrometer. A weak series of $K_{-1} = 0$ *a*-type lines extending from the $2_{02}-1_{01}$ to the $5_{05}-4_{04}$ transition was observed fairly close to the frequencies predicted by the structural model described above for **1a** and **1b**. The intensities of these lines were about a factor of 2 larger than the $K_{-1} = 0$ *a*-type lines assigned to the carbon-13 isotopomers of **1a**. A rigid rotor fit of the measured frequencies of these lines to *B* and *C*, holding the *A* rotational constant fixed at the value obtained from the structural model, was used to better estimate the line positions of the $K_{-1} = 1$ and 2 transitions. The $K_{-1} = 1$ lines were observed for the $J = 2-1$ through $J = 5-4$ *a*-type transitions. It was not possible to observe the $K_{-1} = 2$ transitions presumably due to the low populations of these relatively high energy states in the pulsed beam. The measured frequencies of the fifteen transitions listed in Table 1 were iteratively fit to the asymmetrical top Hamiltonian described above.[12] To fit the lines to the estimated measurement precision of 2 kHz, it was necessary to include the three quartic centrifugal distortion constants, Δ_J, Δ_{JK}, and δ_J. Table 2 lists the spectral constants obtained from this fit. The *A* rotational constant is not well determined and attempts to identify the less intense *b*-type transitions, which have a stronger dependence upon *A*, were not successful.

TABLE 6: Atomic Substitution Coordinates of 1a, (*Z*)-CH_3CH_2CHSO

atom	*a* (Å)[a]	*b* (Å)[a]	*c* (Å)[a]
S	1.212(1)	−0.399(4)	0.128(11)
C_1	−0.296(5)	−0.765(2)	−0.190(8)
C_2	−1.398(1)	0.195(8)	−0.581(3)
C_3	−2.5546(6)	0.208(7)	0.430(3)
H_3	−0.745(2)	1.208(1)	−0.742(2)

[a] The r_s coordinates, *a*, *b*, and *c*, were calculated from Kraitchman equations in the principal axes of the normal isotopomer with moments of inertia obtained from the rotational constants listed in Tables 2 and 5. Costain uncertainties in the r_s coordinates are given in parentheses.

IV. Electric Dipole Moment of 1a

The electric dipole moment of **1a** was determined from measurements of the frequency shifts as a function of applied electric field for the $M_J = 0,1,2$ Stark components of the $3_{03}-2_{02}$ transition, the $M_J = 0$ Stark component for the $3_{12}-2_{11}$ and the $1_{11}-0_{00}$ transitions, and the $M_J = 0,1$ components of the $2_{12}-1_{01}$ transition. The frequency shifts for each Stark transition were plotted as a function of the square of the applied electric field to test for linear second-order behavior.[13] A least-squares fit of all the Stark data using second-order perturbation theory[13] found the dipole components along the principal axes to be $\mu_a = 2.59(2)$ D, $\mu_b = 2.11(2)$ D, and $\mu_c = 0.33(6)$ D, which gives a total electric dipole moment of 3.35(2) D.

V. Molecular Structure

A. 1a, (*Z*)-CH_3CH_2CHSO. The rotational constants and inertial defect of the normal isotopomer of **1a** agree most closely with a skew structure in which the OSC_1C_2 atoms are located in a plane, with the terminal methyl carbon rotated out of the plane by about 120°. Although six isotopic modifications were assigned for **1a**, there is not sufficient moment of inertia data to calculate the 33 unique atomic coordinates required to completely determine the molecular structure. The Kraitchman method[14] was used to obtain substitution atomic coordinates for the sulfur, three carbon, and one methylene hydrogen atoms. The results of the Kraitchman calculations and estimates of the deviations of the substitution coordinates from the equilibrium values using Costain's rule are listed in Table 6.[13] It was possible to determine the signs of the coordinates by comparison to the structural model that was used for the spectral analysis described in section III. Table 7 lists the structural parameters calculated from the substitution coordinates; the uncertainties reported for these parameters are propagated from the Costain uncertainties in Table 6.

An r_0 structure of **1a** was also determined by iteratively fitting the bond distances and bond angles to the experimental second moments of inertia, $P_{aa} = \sum_i m_i a_i^2$, $P_{bb} = \sum_i m_i b_i^2$, and $P_{cc} = \sum_i m_i c_i^2$.[15] By fitting the structural parameters rather than the atomic coordinates to the second moments, it was possible to constrain certain parameters and fit others. Due to the limited number of isotopomers investigated for **1a**, this provided some

TABLE 7: Interatomic Distances (Å) and Angles (deg) of 1a, (*Z*)-CH_3CH_2CHSO

parameter	r_s[a]	r_0[b]	r_s[c]	r_0[d]
r(S−O)		1.470(2)		1.473(2)
$r(C_1-S)$	1.585(6)	1.593(4)		1.578(4)
$r(C_1-C_2)$	1.513(7)	1.515(5)		1.524(5)
$r(C_2-C_3)$	1.536(3)	1.539(2)		1.544(2)
$r(C_2-H_3)$	1.216(7)	1.207(6)	1.088(7)	1.078(5)
$\theta(C_1SO)$		113.7(2)		113.8(2)
$\theta(C_2C_1S)$	126.7(3)	126.2(1)		126.5(1)
$\theta(C_3C_2C_1)$	112.6(4)	112.6(2)		112.4(1)
$\theta(H_3C_2C_1)$	99.9(2)	100.2(3)	108.2(2)	108.1(3)
$\phi(SC_1C_2C_3)$	118.4	118.4(2)		118.3(2)
$\phi(SC_1C_2H_3)$	351.2	351.3(3)	356.9	357.2(4)

[a] The r_s structural parameters were calculated from the atomic coordinates listed in Table 6; the parameter uncertainties are propagated from the Costain uncertainties reported in Table 6. [b] Second moments of the six isotopomers were iteratively fit to the structural parameters; the residuals of the least-squares fit are given in parentheses. [c] These parameters were calculated from Kraitchman coordinates using rotational constants of (*Z*)-$CH_3CHDCHSO$, which were adjusted for bond and torsional shrinkage effects. [d] The shrinkage-adjusted second moments of (*Z*)-$CH_3CHDCHSO$ and the second moments of the other five isotopomers were iteratively fit to the structural parameters to obtain these r_0 parameters.

advantages over the substitution method. The eighteen second moments of the six isotopomers in the normal isotopic frame were fit to the following bond distances and bond angles: r(S−O), $r(C_1-S)$, $r(C_1-C_2)$, $r(C_2-C_3)$, $r(C_2-H_3)$, $\theta(C_1SO)$, $\theta(C_2C_1S)$, $\theta(C_3C_2C_1)$, $\theta(H_3C_2C_1)$, $\phi(SC_1C_2C_3)$, and $\phi(SC_1C_2H_3)$. The atom numbering for the structural parameters of **1a** is given in Figure 1. It was necessary to fix the following parameters in the fit: $r(C_3-H) = 1.100$ Å, $\theta(HC_3C_2) = 111.8°$, $r(C_1-H_1) = 1.077$ Å, $\theta(H_1C_1S) = 117°$, $r(C_2-H_2) = 1.105$ Å, and $\theta(H_2C_2C_1) = 107.2°$. The H_1 parameters are the same as found for (*Z*)-ethanethial *S*-oxide,[4] and the CH_3CH_2 parameters were taken from the known structure of *cis*-propanal.[16] There is good agreement between the substitution structure and the results of this r_0 fit, also listed in Table 7. The overall standard deviation of the fit was 0.006 u·Å^2.

While all the heavy atom parameters are reasonable, $r(C_2-H_3) = 1.216(7)$ Å and $\theta(H_3C_2C_1) = 99.9(2)°$ are quite anomalous. Methylene C−H distances are typically 1.1 Å or less and bond angles for sp^3-hybridized carbon are close to 109°. Initially, the site of deuteration in the molecule was reconsidered; however, the rotational constants calculated for all the other monodeuterated **1a** isotopomers are very different from the experimental constants determined for the deuterated isotopomer. The atomic coordinates calculated in the r_0 fit clearly show that the substitution coordinates from the deuterium isotopomer can only be assigned to isotopic substitution at the H_3 methylene position.

It is known that differences in zero point energies of the C−H and C−D stretching vibrations do not completely cancel in Kraitchman calculations.[17] A correction factor of 4×10^{-3} Å has been used to account for the isotopic shrinkage in the C−H bond upon deuteration. The rotational constants were calculated from the r_0 structure listed in Table 7 both with and without the shrinkage correction applied to the C−H bond length. Differences between these two sets of constants were then added to the experimentally determined constants, and a structure was calculated from the corrected rotational constants.[18] The shrinkage corrections have a negligible effect upon the heavy atom structure and give values of $r(C_2-H_3) = 1.199(6)$ Å and $\theta(H_3C_2C_1) = 100.2(3)°$. These changes are much too small to account for the unusual H_3 structural parameters.

A similar anomaly was observed in structural calculations of *gauche*-propanal, CH_3CH_2CHO.[16] In that work, the nonbonded r_s distance between the oxygen atom and the aldehydic hydrogen was long by 0.1 Å, relative to comparable molecules. It was not possible to calculate the r_s C−H distance because the aldehydic carbon was not isotopically substituted. The authors reasoned that differences in the zero point energies of the CHO torsion upon deuteration resulted in an average CCCH dihedral angle larger than it is for CCCD. An analysis analogous to the isotopic shrinkage described above varied the torsional angle. They found that a correction of ∼0.5° in the torsional angle provided adjusted constants that reduced the nonbonded O···H distance by 0.1 Å to a reasonable value. We found that a torsional shrinkage correction of ∼0.4° combined with a 0.004 Å C−D shrinkage applied to **1a** gave r_0 H_3 parameters of $r(C_2-H_3) = 1.078(5)$ Å, $\theta(H_3C_2C_1) = 108.1(3)°$, and $\phi(SC_1C_2H_3) = 357.2(4)°$, which compare closely to the r_s H_3 parameters listed in column three of Table 7. The entire r_0 structure obtained from the adjusted rotational constants is listed in column four of Table 7. There are small changes in the heavy atom r_0 parameters of the shrinkage-corrected structure compared to the uncorrected r_0 structure. The overall standard deviation is lower for the shrinkage-corrected fit, 0.005 u·Å^2, compared to 0.006 u·Å^2 for the uncorrected fit. Variations in the heavy atom parameters for the Kraitchman and two r_0 analyses give an estimate of the uncertainties due to zero point vibrational effects. However, the best estimates of the structural parameters for the H_3 atom are from the torsion and distance shrinkage analysis.

B. 1b, (*E*)-CH_3CH_2CHSO. There is not sufficient isotopic data to calculate the structural parameters of **1b**, (*E*)-CH_3CH_2CHSO. Rearrangement of the (*Z*)-CH_3CH_2CHSO structure into the (*E*) form using the shrinkage-corrected r_0 parameters listed in Table 7 rather closely predicts the measured rotational constants of (*E*)-CH_3CH_2CHSO. This indicates that there are not large structural differences between the two geometrical isomers. It is possible to obtain a reasonable fit of the three second moments of the normal isotopomer of **1b** to $\phi(SC_1C_2C_3)$ and $\theta(C_2C_1S)$, constraining all the remaining structural parameters to the shrinkage-corrected r_0 parameters for (*Z*)-CH_3CH_2CHSO. This gives an overall standard deviation of 0.006 u·Å^2 with $\phi(SC_1C_2C_3) = 116.84(3)°$ and $\theta(C_2C_1S) = 121.89(2)°$. Since $\phi(SC_1C_2C_3)$ differs by 1.5° between **1a** and **1b**, the major change is a decrease of 4.6° in $\theta(C_2C_1S)$. However, this result is not definitive and more isotopic data are required to unambiguously determine small differences in the structures of the two isomers.

VI. Discussion

The microwave results reported above show that **1**, produced in a (*Z*)/(*E*) ratio of 98/2, and isobutylene are the major products from the pyrolysis of **2** at 350 °C.[3] Since the microwave spectra of the skew rotatomers of **1a** and **1b** are observed, other conformers must be higher in energy and are not populated in the cold gas pulses. In addition, there are no resolvable splittings of the observed rotational transitions of **1a** and **1b**. This indicates that the trans barrier for quantum mechanical tunneling between equivalent forms of the skew rotatomer is high.

Hindered rotation about the C(sp^2)−C(sp^3) bond has been studied for a number of simple molecules by gas-phase microwave spectroscopy.[19] Propanal, 1-butene, and **1** all have a common ethyl side chain and differ by the aldehyde, vinyl, and sulfine functional groups. Both cis and skew forms of propanal[20−23] and 1-butene[24] have been identified from microwave studies. The cis rotatomer of propanal is 420 cm^{-1} more stable than the skew form,[23] while this energy difference is only 26 cm^{-1} for 1-butene.[24] Hence, the cis form is clearly more stable for propanal, the two rotatomers are of similar energy for 1-butene, and the lowest energy form is skew for both geometrical isomers of **1**. Propanal has a low trans internal rotation barrier of 300 cm^{-1}, which gives rise to tunneling splittings in the ground-state spectrum.[23] In 1-butene[24] and **1**, this barrier is considerably higher, and no tunneling splittings are observed.

Wiberg and Martin have used ab initio MO calculations to study the origins of the barriers and the factors involved in the stabilization of the lowest energy form for 1-butene and propanal.[25] They find the barrier in 1-butene is due to overlap repulsion between the C−H bonding orbitals of the adjacent vinyl and methylene CH bonds. A similar C−H overlap repulsion accounts for the origins of the rotational barriers in acetaldehyde, acetone, and propene.[25] The lowest energy conformer of all these compounds has the methyl hydrogen eclipsed with the carbonyl or C=C group. Stabilization of the cis conformer and the rotational barrier of propanal are due to additional terms in the potential that arise from a polarization of the ethyl group C−C bond by the carbonyl CO bond dipole and an overlap of these two bond orbitals.[25]

Ethanethial,[26] **1a,b**, and **3a,b** also have the methyl group or methylene ethyl group C−H bond eclipsed with the adjacent C=O or C=S bond. Restricted Hartree−Fock calculations of **3a,b** found that stabilization of the eclipsed conformations arise from orbital and electrostatic interactions between the methyl hydrogen and the oxygen.[27] The oxygen to eclipsed hydrogen nonbonded distances are found experimentally to be 2.60 and 2.56 Å, respectively, for **3a** and **1a**, which may indicate the presence of weak hydrogen bonds. Three-fold methyl barriers of **3a**, acetaldehyde,[28] and ethanethial[26] have been measured to be 0.8159, 1.16, and 1.57 kcal/mol, respectively. In the case of **3a**, a calculated Hartree−Fock value of 0.8 kcal/mol is in good agreement with the measured barrier.[27] No splittings of the rotational transitions of **1a,b** were observed in the present work so the methyl internal rotor barriers must be high.

Due to the low temperature of the pulsed supersonic beam, the present microwave work on **1a,b** yielded no data on excited vibrational states of the low-lying torsional vibration of the observed skew form. These data as well as rotational assignments of higher energy conformers are needed to obtain information on the potential and rotational barriers of **1a**. A preliminary study of **1a** at room-temperature identified microwave transitions that were assigned to the ground state of the skew conformer.[29,30] It is certain from the spectral assignment listed in Table 1 that the earlier assignment is not correct. However, the transitions measured previously might arise from excited states of the torsional vibration of the skew form and/or from a higher energy conformation. Additional microwave studies of **1a** at room temperature are needed to determine the origin of these lines.

The low temperature of the pulsed supersonic beam offers a reasonable explanation of the presence of only one isotopic spectrum of **1a**, (*Z*)-$CH_3CHDCHSO$. Since the two methylene hydrogens are nonequivalent, rotational spectra of both of these isotopomers should be present. However, small differences in the zero point vibrational energies of the two deuterium isotopomers become significant at the low temperature of the supersonic gas pulses. It appears that in this case, there is not sufficient population of the isotopomer with the deuterium substituted out of the OSCC plane to observe the spectrum in a Ne/He expansion. A similar effect was reported for the monosubstituted and disubstituted deuterium isotopomers of **3a**, (*Z*)-CH_2DCHSO, and (*Z*)-CHD_2CHSO.[4] Spectra for two different d_1-isotopomers were obtained when the backing gas consisted of a Ne/He mixture, one with the deuterium cis to the oxygen, the other with it skew. In a colder argon beam, the d_1-skew isotopomer spectrum was barely visible, which indicates it is the higher energy form. Analagous results were obtained for the d_2-substitution of **3a**, where the isotopomer in which deuterium is cis to the oxygen was again shown to be the lower energy form.

TABLE 8: Comparison of Structural Parameters (Å and deg) of Thial *S*-Oxides

parameter	$HCH{=}S^{+}{-}O^{-}$	**3a** $CH_3CH{=}S^{+}{-}O^{-}$	**1a** $CH_3CH_2CH{=}S^{+}{-}O^{-}$
r(C=S)	1.610(2)	1.618(3)	1.585(6)
r(S−O)	1.469(2)	1.477(4)	1.473(2)
r(=CH−CH$_3$)		1.493(3)	
r(=CH−CH$_2$−)			1.513(7)
r(−CH$_2$−CH$_3$)			1.536(3)
θ(CSO)	114.72(2)	113.9(2)	113.8(2)
θ(CCS)		125.4(2)	126.7(3)
θ(CCC)			112.6(4)
ϕ(CCCS)			118.4
ref	1	4	this work

Table 8 compares the gas-phase geometry of **1a** with its lower homologues, methanethial *S*-oxide ($HCH{=}S^{+}{-}O^{-}$) and **3a**. There is a 0.007 Å difference in the S=O distances of methanethial *S*-oxide and **3a** while the **1a** S=O distance falls between the two. These experimental S=O distances are in fair agreement with an ab initio value of 1.466 Å computed for **3a**.[31] In comparison to the parent sulfine, methanethial *S*-oxide, the C=S distance is 0.008 Å larger for **3a** and 0.025 Å smaller for **1a**. This apparent anomaly finds no explanation in the ab initio study of **3a** where the computed C=S distance (1.593 Å) is close to the experimental value of **1a** (1.585 Å) rather than **3a** (1.618 Å).[31] It may in part arise from difficulties in the Kraitchman calculation of the carbon coordinates of **1a** due to torsional shrinkage effects discussed in the structure section. However, $r(-CH_2-CH_3) = 1.536$ Å and $r(=CH-CH_2-) = 1.513$ Å of **1a** are reasonable when compared to these same bond distances in 1-butene and propanal.[22,24]

Acknowledgment. We gratefully acknowledge support from the donors of the Petroleum Research Fund, administered by the American Chemical Society (J.Z.G.), and the National Science Foundation (J.Z.G. and E.B.)

References and Notes

(1) Penn, R. E.; Olsen, R. J. *J. Mol. Spectrosc.* **1976**, *61*, 21.

(2) Block, E. *Angew. Chem., Int. Ed. Engl.* **1992**, *31*, 1135.

(3) Block, E.; Gillies, J. Z.; Gillies, C. W.; Bazzi, A. A.; Putman, D.; Revelle, L. K.; Wang, D.; Zhang, X. *J. Am. Chem. Soc.* **1996**, *118*, 7492.

(4) Gillies, J. Z.; Gillies, C. W.; Grabow, J.; Hartwig, H.; Block, E. *J. Phys. Chem.* **1996**, *100*, 18708.

(5) Gillies, J. Z.; Gillies, C. W.; Lovas, F. J.; Matsumura, K.; Suenram, R. D.; Kraka, R. D.; Cremer, D. *J. Am. Chem. Soc.* **1991**, *113*, 6408.

(6) Scharpen, L. H.; Laurie, V. W. *J. Chem. Phys.* **1963**, *39*, 1732.

(7) Warner, H. E.; Wang, Y.; Ward, C.; Gillies, C. W.; Interrante, L. *J. Phys. Chem.* **1994**, *98*, 12215.

(8) Balle, T. J.; Flygare, W. H. *Rev. Sci. Instrum.* **1981**, *52*, 33.

(9) Coudert, L. H.; Lovas, F. J.; Suenram, R. D.; Hougen, J. T. *J. Chem. Phys.* **1987**, *87*, 6290.

(10) Boyce, C. W.; Gillies, C. W.; Warner, H.; Gillies, J. Z.; Lovas, F. J.; Suenram, R. D. *J. Mol. Spectrosc.* **1995**, *171*, 533.

(11) Reinhartz, J. M. L. J.; Dynamus, A. *Chem. Phys. Lett.* **1974**, *24*, 346.

(12) Watson, J. K. G. In *Vibrational Spectra and Structure*; Durig, J. R., Ed.; Elsevier: Amsterdam, 1977; Vol. 6, p 1.

(13) Gordy, W.; Cook, R. L. *Microwave Molecular Spectra*; John Wiley & Sons: New York, 1984.

(14) Kraitchman, J. *Am. J. Phys.* **1953**, *21*, 17.

(15) Harmony, M. D.; Laurie, V. W.; Kuczkowski, R. L.; Schwendeman, R. H.; Ramsay, D. A.; Lovas, F. J.; Lafferty, W. J.; Maki, A. G. *J. Phys. Chem. Ref. Data* **1979**, *8*, 619.

(16) Randell, J.; Cox, A. P.; Hillig, K. W.; Imachi, M.; LaBarge, M. S.; Kuczowski, R. L. *Z. Naturforsch.* **1987**, *43A*, 271.

(17) Laurie, V. W.; Herschbach, D. R. *J. Chem. Phys.* **1962**, *37*, 1687.

(18) Schwendeman, R. H. Structural Parameters from Rotational Spectra. In *Critical Evaluation of Chemical and Physical Structural Information*; Lide, D. R., Paul, M. A., Eds.; National Academy of Science: Washington, DC, 1974.

(19) Wilson, E. B. *Chem. Soc. Rev.* **1972**, *3*, 293.

(20) Butcher, S. S.; Wilson, E. B. *J. Chem. Phys.* **1964**, *40*, 1671.

(21) Pickett, H. M.; Scroggin, D. G. *J. Chem. Phys.* **1974**, *61*, 3954.

(22) Randell, J.; Cox, A. P.; Hillig, K. W., II; Imachi, M.; LaBarge, M. S.; Kuczkowski, R. L. *Z. Naturforsch.* **1988**, *43A*, 271.

(23) Randell, J. R.; Hardy, J. A.; Cox, A. P. *J. Chem. Soc., Faraday Trans. 2* **1988**, *84*, 1199.

(24) Kondo, S.; Hirota, E.; Morino, Y. *J. Mol. Spectrosc.* **1968**, *28*, 471.

(25) Wiberg, K. B.; Martin, E. *J. Am. Chem. Soc.* **1985**, *107*, 5035.

(26) Kroto, H.; Landsberg, B. M. *J. Mol. Spectrosc.* **1976**, *62*, 346.

(27) Block, E.; Penn, R. E.; Bazzi, A. A.; Cremer, D. *Tetrahedron Lett.* **1981**, *22*, 29.

(28) Kilb, R. W.; Lin, C. C.; Wilson, E. B. *J. Chem. Phys.* **1957**, *26*, 1695.

(29) Block, E.; Penn, R. E.; Revelle, L. K. *J. Am. Chem. Soc.* **1979**, *101*, 2200.

(30) R. E. Penn left The University of Missouri at St. Louis to take a position with The DuPont Chemical Co. and did not publish the primary microwave data on **1a** that provided the experimental support for ref 29.

(31) Turecek, F.; McLafferty, F. W.; Smith, B. J.; Radom, L. *Int. J. Mass Spectrom. Ion Processes* **1990**, *101*, 283.